Correction of aberrant axon growth in the developing mouse olfactory bulb

Caroline Chan[1,2], Jenny A. K. Ekberg[1], Katie E. Lineburg[1], Susan E. Scott[1], Fatemeh Chehrehasa[1], Louisa C.E. Windus[1,2], Christina Claxton[2], Alan Mackay-Sim[1], Brian Key[2], James A. St John[1]

[1]National Centre for Adult Stem Cell Research, Eskitis Institute for Cell and Molecular Therapies, Griffith University, Nathan, Brisbane 4111, Queensland, Australia

[2]School of Biomedical Sciences, The University of Queensland, Brisbane 4072, Queensland, Australia.

*Correspondence to: Dr James St John, National Centre for Adult Stem Cell Research, Eskitis Institute for Cell and Molecular Therapies, Griffith University, Nathan, Brisbane 4111, Queensland, Australia; Telephone +61-7-3735 3660; Fax +61-7-3735 4255; e-mail: j.stjohn@griffith.edu.au

Abstract

During development of the primary olfactory system, sensory axons project from the nasal cavity to the glomerular layer of the olfactory bulb. In the process axons can branch inappropriately into several glomeruli and sometimes over-shoot the glomerular layer, entering the deeper external plexiform layer. However in the adult, axons are rarely observed within the external plexiform layer. While chemorepulsive cues are proposed to restrict axons to the glomerular layer in the embryonic animal, these cues are clearly insufficient for all axons in the postnatal animal. We hypothesised that the external plexiform layer is initially an environment in which axons are able to grow but becomes increasingly inhibitory to axon growth in later postnatal development. We have determined that rather than having short localised trajectories as previously assumed, many axons that enter the external plexiform layer had considerable trajectories and projected preferentially along the ventro-dorsal and rostro-caudal axes for up to 950 μm. With increasing age, fewer axons were detected within the external plexiform layer but axons continued to be present until P17. Thus the external plexiform layer is initially an environment in which axons can extensively grow. We next tested whether the external plexiform layer became increasingly inhibitory to axon growth by microdissecting various layers of the olfactory bulb and preparing protein extracts. When assayed using olfactory epithelium explants of the same embryonic age, primary olfactory axons became increasingly inhibited by extract prepared from the external plexiform layer of increasingly older animals. These results demonstrate that primary olfactory axons can initially grow extensively in the external plexiform layer, but that during postnatal development inhibitory cues are upregulated that reduce axon growth within the external plexiform layer.

Key words: neuron; glomerulus; external plexiform layer; repulsion; glomerular layer; ZsGreen

1. Introduction

Primary olfactory neurons that express the same odorant receptor are mosaically distributed within the olfactory neuroepithelium and appear to have no particular spatial relation to each other (Ressler et al., 1993; Vassar et al., 1994). Despite this distribution, primary olfactory axons arising from these neurons are able to sort out, fasciculate together and target glomeruli to form the highly specific and topographically fixed olfactory map (Mombaerts, 1996; Ressler et al., 1994; Royal and Key, 1999; Treloar et al., 2002; Vassar et al., 1994). The development of this complex projection pattern involves the migration of numerous cell types and the extension of their processes into different layers of the olfactory bulb. While the timing of many events is coincident with the appearance of glomeruli, the cellular interactions driving the formation of this unique synaptic neuropil remain to be determined. We have reported that numerous sensory axons exhibit exuberant growth and project aberrantly into deeper layers of the olfactory bulb during development (Royal and Key, 1999; Tenne-Brown and Key, 1999). Others have instead noted the specificity with which primary olfactory axons are able to home to their target and form glomeruli without the need for error correction (Dynes and Ngai, 1998; Klenoff and Greer, 1998; Potter et al., 2001; Treloar et al., 2002; Wang et al., 1998).

There is no generic mechanism that governs the development of topographic connections in different neural pathways. In the visual system, retinal axons initially form a diffuse map on the tectum which is subsequently refined into a strict topography as a result of pruning and lateral branching (Hindges et al., 2002; Simon and O'Leary, 1992; Yates et al., 2001). In contrast, dorsal root sensory axons establish

a correct topographic map in the dorsal horn of the spinal cord as the pathway forms (Silos-Santiago et al., 1995). Dorsal root axons always grow specifically to their target lamina without branching or over-shooting into inappropriate regions in the dorsal horn (Ozaki and Snider, 1997). The extent of error formation by sensory axon projections in the olfactory bulb and the cues that lead to their removal still remains to be resolved.

During development in the olfactory nerve pathway, while many axons project directly to a glomerulus (Dynes and Ngai, 1998; Klenoff and Greer, 1998; Potter et al., 2001; Treloar et al., 2002; Treloar et al., 1999; Wang et al., 1998) it is clear that many axons make errors in targeting, branch into numerous glomeruli, and can over-project past the target layer into the deeper layers of the olfactory bulb (Royal and Key, 1999; Santacana et al., 1992; Tenne-Brown and Key, 1999). The development of P2-odorant glomeruli in mice commences around embryonic day 14.5 (E14.5) when P2 axons coalesce in a broad locus underlying the presumptive glomerular layer (Royal and Key, 1999). Over the next 5 days the axons develop into discrete glomerular structures. During this period the P2-odorant receptor axons are intermingled with other odorant receptor axons, branch into neighbouring glomeruli and project into deeper layers of the olfactory bulb. It is not until postnatal day 7.5 that P2 glomeruli become distinct and separate, with all axons terminating within the target glomeruli (Royal and Key, 1999). This initial inaccuracy of targeting is not restricted to P2 axons, but is typical of the majority of axons. Tenne-Brown and Key (1999) reported that at P1.5, 54% of axons did not terminate directly in a glomerulus, and that 22% of axons projected aberrantly into the external plexiform layer. However, axons were reported to project directly to their glomerular target by P5.5.

Similarly in rat, aberrant projections into the external plexiform layer have been observed up to P9 (Royal and Key, 1999). Thus the mechanisms that regulate axonal targeting are not precise and many axons are not initially successful in recognising their target glomeruli.

We hypothesised that the external plexiform layer is initially an environment in which axons are able to grow, but becomes increasingly inhibitory with later development. In the present study we addressed this issue and found that in early postnatal animals, many sensory axons are able to enter the external plexiform layer and are capable of growing tangentially for long distances where they form a diffuse plexus. We then examined axon outgrowth from olfactory epithelial explants obtained from the same embryonic age animals and found that with increasing developmental age, the external plexiform layer becomes increasingly repulsive to primary olfactory axons. These results show that the external plexiform layer contributes to restricting primary olfactory axons to the superficial layers of the olfactory bulb.

2. Material and methods

2.1 OMP-ZsGreen transgenic mice

Transgenic mice expressing ZsGreen in olfactory sensory neurons were previously generated (Windus et al., 2010). ZsGreen is a reef coral fluorescent protein derived from the Anthozoa class of non-bioluminescent reef corals that exhibit bright fluorescent colours. This protein has been adapted to use as in vivo reporter by introduction of a series of mutations into the full-length cDNA (Matz et al., 1999; Wenck et al., 2003). In these mice, the full length (5.5kb) OMP promoter (Danciger et al., 1989) drove the expression of ZsGreen fluorescent protein, from pZsGreen-Express Vector (Clontech, Palo Alto, CA).

2.2 Methimazole treatment

Methimazole (Sigma-Aldrich, catalog number M8506) was prepared at a concentration of 10 mg/mL phosphate buffered saline and injected intraperitoneally into adult OMP-ZsGreen transgenic mice at a concentration of 50 mg/kg body weight; control mice were injected with PBS alone. The mice were returned to their cages and three mice at each time point were sacrificed at 3, 7, 14 and 21 days after the injection.

2.3 Tissue preparation

Quackenbush Swiss mice or OMP-ZsGreen transgenic mice were time plugged and the day of positive sperm dam was designated E0.5. Tissue was collected from mice at various postnatal days (P) and from adult animals. At least three animals were examined at each age. Postnatal mice younger than P10 were killed by decapitation;

older mice were killed by cervical dislocation and heads were immersion-fixed for 24 hr at 4 ºC in 4% paraformaldehyde in phosphate buffered saline (PBS; pH 7.4). Following fixation, postnatal heads up to P5.5 were cryoprotected in 30% sucrose with 0.1% sodium azide. Heads older than P8.5 were decalcified in 20% disodium ethylene diaminetetraacetic acid in PBS (pH 7.4). Heads were placed in embedding matrix (O.C.T. compound, Miles Scientific, Naperville, IL) and snap frozen by immersion in iso-pentane that had been cooled by liquid nitrogen.

Serial coronal sections (30 μm) were cut on a cryostat microtome and mounted on glass slides. Serial parasagittal cryostat sections (100 μm) from postnatal and adult animals were cut and were transferred into a petri dish containing ice-cold Tris-buffered saline (TBS; pH 7.4). Following immunohistochemistry (described below), the free-floating sections were mounted on slides coated with 2% gelatine and 0.1% chromalum. All procedures were carried out with the approval of, and in accordance with, the Griffith University Animal Ethics Committee and the University of Queensland Animal Ethics Experimentation Committee.

2.4 Preparation of olfactory epithelium explant culture

Timed pregnant OMP-ZsGreen mice were sacrificed by 5% CO_2 gas asphyxiation and E14.5 embryos were decapitated. Olfactory epithelium was dissected from the nasal septum and the underlying lamina propria was removed using superfine forceps. The explant was plated on Matrigel basement membrane matrix (BD Bioscience, product number 356234, 1:10) coated on glass bottom cell culture dish.

2.5 Preparation of olfactory bulb slices and extract

P2.5, P8.5 and P17.5 mice were sacrificed by decapitation. The skull was removed from the animal head to expose the olfactory bulb and cortex. The whole olfactory bulb with a portion of cortex was placed in a flat bottom plastic mould containing warm 3% low melting point agarose. Thick coronal slices of olfactory bulb (100 μm) were cut with a vibratome (Microm international) and placed in cold neurobasal medium containing 5 μg/ml gentamycin. Under a stereomicroscope, the different layers of the olfactory bulb slices were dissected using superfine forceps. The nerve fiber layer was removed and discarded. The glomerular layer was separated from the external plexiform layer of P17.5 animals and retained. The inner layer of the olfactory bulb consisting of the external plexiform layer, mitral cell layer together with internal plexiform layer was dissected out from all ages and retained; and tissue from the frontal cortex adjacent to the olfactory bulb was also collected. The dissected layers from the olfactory bulb, and tissue from the frontal cortex, were placed in separate eppendorf tubes containing 30 μl CM placed on ice and additional CM was added on a 5 ml per g basis. Thus the ratio of the mass of tissue to medium (g/mL) was the same for all ages examined. The tissue was lysed by pipetting up and down and passing through 27G-30G needle multiple times. Before addition to the olfactory epithelium explants, the extract was collected by centrifugation at 15000 rpm for 15 min at 4 ^{o}C. For controls, extract was heat inactivated (70 ^{o}C for 20 min). Extract was added to the olfactory epithelium explant at 1:4 dilution in CM. Experiments were repeated 3 times, with at least 2-3 explants being analysed in each experiment; numbers of explants analysed are detailed in the legend for Figure 8. Times lapse images were collected for up to 4.5 hr (30 min before addition of extract and 4 hr after addition of extract) at intervals of ~4 min using an inverted Zeiss Axiovert 200 live cell imaging microscope fitted with a 37 ^{o}C heated stage, 5% CO_2, epifluoresecence

and a Zeiss axiocam digital camera. Images taken immediately prior to addition of the extract (30 min after imaging commenced) were determined to be time 0. After 12 hr incubation, explants were fixed with 4% PFA for 30 min and images taken using confocal microscopy.

2.6 Immunohistochemistry

To enhance OMP antibody detection of the over-projecting axons, immunohistochemistry was performed on free floating 100 μm thick cryostat sections using a protocol developed for immunostaining wholemount zebrafish embryos (Devine and Key, 2008). The sections were incubated for 5 min with 0.05% H_2O_2 in methanol to inhibit endogenous peroxidase activity and then blocked with 2% bovine serum albumin (BSA; Sigma Chemical Corporation) with 0.3% Triton X-100 (TX-100) in 0.1 M Tris-buffered saline (TBS), pH 7.4. Sections were then incubated overnight at 4 °C with goat polyclonal antiserum against olfactory marker protein (OMP) at 1:30,000 (Keller and Margolis, 1975), followed by biotinylated rabbit anti-goat immunoglobulin antibodies (1:400; Vector Laboratories Incorporated, Burlingame, CA) for 4 hr at 4 °C and then avidin-biotin-horseradish peroxidase (Vectastain Elite ABC kit; Vector) for 1 hr at room temperature. Some sections were stained with the lectin *Dolichos biflorus* agglutinin (DBA) followed by avidin-biotin-hrp. Staining was visualised by reaction with diaminobenzidine and H_2O_2 in TBS. For fluorescence immunohistochemistry on 30 μm thick cryostat sections, the sections were blocked with 2% BSA with 0.3% TX-100 in 0.1 M TBS and then incubated overnight at 4 °C with goat polyclonal antiserum against OMP at 1:5,000 followed by Alexa-fluor 594 donkey anti-goat immunoglobulin antibodies (Invitrogen Catalog number A-11058). Images were taken using confocal microscopy.

2.7 Microscopy and Image preparation

Images were collected with a Spot 2 digital camera (Spot Diagnostic Instruments, Inc., Sterling Heights, MI) fitted on an Olympus BH2 microscope with differential interference contrast optics; or with a Zeiss apotome microscope; or with an Olympus FV-1000 confocal microscope. Images were colour balanced and cropped using Adobe Photoshop 7.0 and Figures were prepared using Adobe Illustrator 10 (Adobe Systems, CA).

2.8 Quantification of axon density and axon length in vitro

The area covered by axons within the EPL was quantified using ImageJ software by binarising the images of the axons within the EPL and then measuring the area covered by the axons in comparison to the total area of the EPL in the field of view. For this experiment, 10,000 μm^2 areas of the EPL in 10 cryostat sections from each of 3 animals were examined. The length of primary olfactory axon outgrowth from the olfactory epithelium explant was determined using the FilamentTracer function of the Imaris analysis software (Bitplane Scientific Solutions). As the axons tended to grow in fascicles we measured the lengths of all fascicles as well as the few individual axons that we could detect. The lengths of axons were determined at time zero which was immediately prior to the addition of the EPL extract or candidate repellent molecules. The change in axon length was determined in comparison to the length of axons at time 0. Thus after addition of the treatment of the explants, axons that did not change length had a 0% change, axons that became longer had a positive change, and axons that became shorter had a negative change. All measurements for each explant were obtained prior to and after the addition of the treatment; this took into account

any variabilities in axon lengths that may occur due to size and extent of initial outgrowth from each explants. Statistical analysis of the change in axon length was carried out using Graphpad Prism 5 (Graphpad Prism, Inc) using a Kruskal-Wallis test and post-hoc Dunnnett's Multiple Comparison test.

2.9 Quantification of axon length in vivo

Cryostat sagittal and coronal sections (30 μm) through the external plexiform layer of OMP-ZsGreen mice (3 animals at each age and for each plane of sectioning) were coverslipped and imaged using confocal microscopy. The Olympus FV1000 software was used to measure (i) the length of axons with a trajectory within the EPL both within coronal and sagittal sections, (ii) the breadth of the EPL in the coronal plane by measuring the distance from the glomerular layer to mitral cell layer, and (iii) the breadth of the EPL in parasagittal sections by measuring the distance from the ventral glomerular layer to the dorsal glomerular layer taken perpendicular to the mid point of the rostral-caudal distance of the ventral glomerular layer. For the lengths of axons, the five longest individual axons in each of at least 5 sections were measured; some sections had fewer than 5 clearly individual axons. Statistical analysis was performed using Graphpad Prism 5 using a using a Kruskal-Wallis test and post-hoc Dunnnett's Multiple Comparison test.

Methimazole

50 μg/g body weight injected as 15 μl (20 mg/ml) in 3 day old pups. Harvested 7 days later at P10.

3. Results

3.1 Primary olfactory axons have extensive trajectories in the external plexiform layer

Previous studies have revealed that during development many primary olfactory axons aberrantly project past their target, the glomerular layer, and continue into the deeper external plexiform layer (EPL) of the olfactory bulb (Bailey et al., 1999; Graziadei et al., 1980; Key and Akeson, 1993; Santacana et al., 1992; Tenne-Brown and Key, 1999; Treloar et al., 1996). This exuberant radial growth may be a consequence of the inability of some growth cones to recognize appropriate stop signals (Poeck et al., 2001) in the glomerular layer. If this was the case then once axons have entered the EPL they may grow unchecked. However, over-projecting axons have been noted to loop in the EPL and then turn back towards the glomerular layer, suggesting that the EPL is non-conducive for primary olfactory axon growth (Treloar et al., 1997; Treloar et al., 2002). We were interested in determining the extent of primary olfactory axon growth within the EPL. Do primary olfactory axons only project a short distance into the EPL and then return to the glomerular layer or do they find the EPL a region in which they can continue to extend?

Our initial analysis of coronal sections from early neonatal bulbs confirmed that primary olfactory axons do project deep past the glomerular layer and into the underlying EPL, with some even projecting into the internal plexiform layer (Fig. 1A, B). Immunostaining for the olfactory marker protein (OMP) revealed numerous axons coursing radially within the EPL. While many axons were observed looping back as if they were repelled by the mitral cell layer, there was considerable granular or punctate staining of the EPL which suggested the presence of transversely-

sectioned axons (Fig. 1B). In coronal sections, it is difficult to determine the trajectory of axons that have turned and grown tangentially within this layer. We addressed this question by examining thick (100 μm) parasagittal sections of the olfactory bulb. Flat-mounts of the EPL on the medial and lateral surfaces of the bulb were present in some of these sections (Fig. 1C, D), enabling us to examine the extent of the trajectory of axons as they coursed tangentially within this layer. These thick parasaggital sections clearly revealed the extent to which the primary olfactory axons projected into the EPL and formed a loose and extensive network throughout this layer (Fig. 1E-F, Fig. 2). OMP stained axons appeared to extend throughout the ventral-dorsal breadth of the bulb at postnatal day (PD) 0.5 (Fig. 1E). However, because of the extent of this exuberant growth it was not possible to trace the trajectory of axons past the midpoint in the dorsoventral axis (Fig. 1F). This is probably why they were previously not recognized in coronal sections of the bulb and explains the granular staining in the EPL (see Fig. 1B). While in parasagittal sections these deeper growing axons appear to be confined to the middle one-third of the bulb (see arrows in Fig. 1E-F) this is actually because it is not possible to obtain the entire rostrocaudal extent of the EPL within a single parasagittal section. In older animals, primary olfactory axons continued to project into and grow tangentially within the EPL (Fig. 2A-B). Since there were fewer axons exhibiting this growth in these animals it was possible to trace the trajectory of single axons or small fascicles over considerable distances in the EPL (Fig. 2C-E). Axons projected over half the dorso-ventral width of the postnatal olfactory bulb, and in some cases they were observed to extend for around 950 μm (Fig. 2D). We were unable to follow the entire trajectory of individual axons that were within the EPL since they often eventually disappeared out the plane to the section, or they intermingled with other axons. However, close examination of individual axons

revealed that they appeared to have few, if any, branches for at least several hundred microns and had a somewhat tortuous wandering trajectory (Fig. 2D).

3.2 Axons form an extensive network

To further investigate the nature of the axon trajectories within the EPL we next examined axon trajectories within parasagittal sections that passed through the middle portion of the olfactory bulb (see small dotted line in Fig. 1D). In these sections the laminae are organized similarly to those in coronal sections; there is a glomerular layer, an EPL and a mitral cell layer and a deeper inner granule cell layer (Fig. 3A). The major difference is in the orientation of the EPL. In this case axons coursing longitudinally along the rostrocaudal axis will be clearly observed. As expected, we identified over-shooting axons that could only be traced for a short distance either rostrally or caudally in the EPL (Fig. 3A,B, D,E). This is consistent with our observations that over-shooting axons course obliquely as well as dorsoventrally when viewed in parasagittal sections taken through the medial and lateral regions of the olfactory bulb (see Fig. 1E). Thus, in sections through the middle region of the bulb over-shooting axons coursed briefly either rostrally or caudally before passing out of the plane of section as they projected ventrally or dorsally in the EPL.

3.3 The lectin, DBA, labels deep projecting axons of the AOB

The lectin, *Dolichos biflorus* agglutinin, labels a large subpopulation of primary olfactory axons and strongly labels all primary axons of the accessory olfactory system (Key and Akeson, 1993). Since OMP is not as strongly expressed by accessory olfactory axons we used the lectin DBA to determine whether these axons also over-shot their target, as in the main olfactory system. Deep projecting accessory

olfactory axons were clearly labelled by DBA coursing in the plexiform layer of the accessory olfactory bulb (Fig. 3C, F). These over-shooting axons were not observed at P11.5.

3.4 Axons over-project up until P17

While OMP immunostaining provided strong staining of primary olfactory axons, we suspected that limits to the sensitivity of the technique prevented us from detecting all over-projecting axons. We therefore examined OMP-ZsGreen transgenic mice which express the strongly fluorescent protein ZsGreen under the control of the OMP promoter (Windus et al., 2010). In these mice, the vast majority of primary olfactory neurons throughout the olfactory epithelium express the ZsGreen protein (Fig. 4A). The ZsGreen protein is present throughout the length of the axons of the primary olfactory neurons and is clearly visible within the glomerular layer of the olfactory bulb (Fig. 4B-C). The only cells within the olfactory system that expressed ZsGreen were primary olfactory neurons. Neurons that immunostained with anti-OMP antibodies (Fig. 4E) also expressed ZsGreen (Fig. 4D). Immature primary olfactory neurons were also observed that expressed lower levels of ZsGreen protein (arrow Fig. 4D) but which had very low levels of antibody immunostaining (arrow Fig. 4E). Secondary-only negative control revealed no non-specific binding within the olfactory mucosa (Fig. 4G). Within the olfactory bulb, the ZsGreen colocalised with anti-OMP immunostaining of axons (Fig. 4H-K). Secondary-only negative control revealed no non-specific binding within the glomerular layer and EPL (Fig. 4K). However it was apparent that the ZsGreen expression was considerably stronger than OMP antibody immunofluorescence and thus more detail of the axon trajectory was observed using ZsGreen fluorescence (Fig. 4H, arrow in 4J). Thus we further explored the extent of

primary olfactory axon over-projection by taking advantage of the strong expression of ZsGreen protein in olfactory axons in the OMP-ZsGreen mice. The trajectories of the primary olfactory axons in the OMP-ZsGreen transgenic mice were easily visualised with exquisite detail and confirmed the OMP antibody immunohistochemistry results shown in Figs. 1-3. In parasagittal sections of P2.5 OMP-ZsGreen mice, over-shooting axons were detected within the EPL and the axons followed an oblique trajectory with a caudal and/or dorsal orientation (Fig. 5A-C), however the numerous axons at this age overlapped and intermingled which made it difficult to follow individual axons for any substantial distance. However, in older animals, individual axons with extensive trajectories were frequently detected (Fig. 5D-F). Some of these axons displayed a distinct rostral-caudal trajectory (Fig. 5F), however others also projected in the ventral-dorsal plane and had meandering trajectories which sometimes looped back (arrow, Fig. 5E). Even at this age, there were often numerous axons in close proximity to each other which made it difficult to discern the extent of the trajectories of individual axons (Fig. 5F). In comparison, when viewed in coronal sections at the same age (P7), axons that over-projected into the EPL appeared to have much smaller trajectories and the apparent preference for direction of the trajectories was towards the mitral cell layer (Fig. 5G). By P17, there were fewer axons that over-projected into the EPL, however for those that did it was clear that individual axons as well as axons in small fascicles continued to extend over large distances within the EPL (Fig. 5H-I). We quantified the density of axons that were present within the EPL by determining the percentage area covered by the axons in the early postnatal period (Fig. 5J). In P2 animals, the axons within the EPL covered 6.5% of the EPL area whereas in P7 animals the axons occupied a

significantly smaller proportion of the EPL (3.4% of the EPL, $p<0.001$). Thus there was a dramatic loss of axons from the EPL between P2 and P7.

Due to the easy visualisation of overprojecting axons in the OMP-ZsGreen mice, we quantified the extent of the trajectories in P2 and P7 animals by measuring the continuous length of axons that were visible within the section. However, the axons often projected out of the plane of the section and while it was sometimes possible to track the axons into adjacent sections, we were not confident that we were imaging the same axon due to the proximity of other axons (see Fig. 5G-H). Thus we were unable to measure the entire length of individual axons within the EPL and hence our measurements of the length of axons are likely to be conservative. In addition, in P2.5 animals, only axons that were clearly visualised as being individual axons were measured and hence many of the numerous overlapping axon trajectories were not measured. We performed the measurements in 30 μm-thick sections as this thickness is more commonly used by other researchers and would be more relevant than the measurements in 100 μm-thick sections.

In the coronal plane, axons in P2 animals had a median trajectory length of 93 μm, with some axons extending for up to 168 μm, whereas in P7 animals the median trajectory was 115 μm with a maximum of 237 μm (Fig. 5K). In these coronal sections, the average width of the EPL was 71 μm and 123 μm in P2 and P7 animals, respectively. Thus when viewed in the coronal plane, the apparent extent of the axon trajectories was similar to the visible width of the EPL (Fig. 5K).

When viewed in parasagittal sections of the EPL, the lengths of the axons were significantly longer at both ages ($p<0.001$). In P2 animals the median axon length was 238 μm with some axons extending up to 633 μm (Fig. 5K); and in P7 animals the median axon length was 286 μm with the longest axons being up to 930 μm (Fig. 5K).

To gauge the extent of the trajectories in comparison to the size of the olfactory bulb, we measured the height of the EPL from the ventral glomerular layer to the dorsal glomerular layer in the parasagittal sections of the EPL (see Fig. 1E). This distance was therefore equivalent to the height of the olfactory bulb internal to the glomerular layer. The median height of the EPL was 891 μm in P2 animals and was 1156 μm in P7 animals (Fig. 5K). Thus the median axon had a trajectory within the EPL of 27 and 28% of the internal height of the EPL in P2 and P7animals, respectively, whereas the longest axons had a trajectory of 71% and 80% of the internal height of the EPL in P2 and P7 animals, respectively.

In summary, when viewed in the coronal plane, the axons that entered the EPL had the appearance of having short, localised trajectories that were limited to the visible width of the EPL. In contrast, when viewed in the sagittal plane, the EPL covered the internal breadth of the olfactory bulb and the median length of the longest continuous visible axons were 2.5 fold longer, with the longest axons being 3.9 fold longer, than axons viewed in the coronal plane. The axons with long trajectories within the EPL extended for about 25% of the height of the olfactory bulb with some axons extending for up to 70-80% of the height of the olfactory bulb. Thus axons that enter the EPL can extend for up to almost the entire breadth of the internal olfactory bulb.

3.5 Axons do not over-project following widescale degeneration of the olfactory epithelium

In normal healthy adult mice, over-projecting axons are not detected, but we hypothesised that if there was widespread degeneration followed by regeneration of primary sensory neurons then the subsequent mass in-growth of new axons into the olfactory bulb may lead to axons over-projecting into the EPL. We therefore examined whether over-projection of primary olfactory sensory axons occurs following widespread degeneration of the olfactory epithelium in adult mice. We treated adult OMP-ZsGreen mice with intraperitoneal injection of methimazole which results in the temporary degeneration of the majority of the olfactory epithelium, including the primary olfactory neurons and supporting cells (Brittebo, 1995). Three days following administration of methimazole, the apical layer of the olfactory epithelium had shed off into the nasal cavity leaving behind the basal layer in which the olfactory stem cells reside (Fig. 6A). Within the next few days, the epithelium was rapidly repopulated by supporting cells and new neurons (Fig. 6B-C) and by 21 days after treatment the olfactory epithelium had regained its normal appearance (Fig. 6D). We closely examined the EPL for over-projecting axons in these methimazole treated mice, but at no stage did we observe axons within the EPL (Fig. 6E-H).

3.6 External plexiform layer inhibits axon growth in vitro

The analyses of the axon trajectories have shown that the over-projection of primary olfactory axons into the EPL was reduced over time, and did not occur in the adult following widespread regeneration of the olfactory epithelium. Thus it was hypothesized that either the EPL was initially attrractive for the growth of some axons or that repulsive axon guidance molecules were up-regulated in the EPL during later

development. To test this postulate, an explant culture assay was employed in which primary olfactory axons were cultured with protein extracts derived from different layers of the olfactory bulb. Olfactory epithelium explants were cultured from E14.5 OMP-ZsGreen embryos on Matrigel-coated glass bottom dishes using protocols that were developed and optimized for this project. At day 2 in vitro, numerous axon processes were visible extending from the explants (Fig. 7A) and axon growth continued over the next few days when maintained in normal culture conditions. To evaluate whether the inner layers of the olfactory bulb contained any attractive or repulsive activity to primary olfactory axons, vibratome slices of the olfactory bulb were prepared and the nerve fibre layers and glomerular layers were removed from the slice. The inner layers of the olfactory bulb containing the external plexiform layer, mitral cell layer and internal plexiform layer were then microdissected. The protein extract was prepared using the same mass of EPL tissue per mL for each age examined. This extract from the inner layers of the olfactory bulb will be referred as EPL extract. The EPL extract was then added to the cultured explants at day 2 post-culture. By using the same age of olfactory mucosa explant, but extracts from different aged animals, the assay would detect if repulsive axon cues were present in the different EPL extracts.

We first examined EPL extract derived from P17.5 animals as it is at this stage that fewer axons are observed over-projecting into the EPL compared to the younger ages and thus the presence of a repulsive molecule is most likely to be detected at this age. Prior to addition of the EPL extract, the olfactory epithelium explants exhibited rigorous and extensive axon outgrowth (Fig. 7A). After 12 hr incubation with P17.5 EPL extract (Fig. 7B), axons collapsed (closed arrow) and axon outgrowth was

significantly inhibited. In comparison, explants that were incubated in control medium only (Fig. 7C-D), or with an extract from the glomerular layer of P17 animals (data not shown, but quantification shown in Fig. 8), or with extract from the frontal cortex of P17 animals (Fig. 7G-H) had increased axon outgrowth over the same period. To demonstrate that the conditions of the EPL extract assay did not induce a non-specific response on axon outgrowth (Bagnard et al., 2001; Kapfhammer et al., 2007), the extract was heat treated at 70 ^{o}C for 20 min to inactivate the repellent activity present in the extract. Explants that were incubated with the heat inactivated P17.5 EPL had increased axon growth over the assay period (Fig. 7E-F) which demonstrates that the inhibited axon growth seen by the addition of P17.5 extract (Fig. 7B) was not due to non-specific responses arising from the experimental conditions. These results indicate that the large response observed in the EPL extract was likely due to the activity of a molecule that reduced axon extension.

As numerous primary olfactory axons do over-project during the early postnatal period, it was postulated that the EPL would be less inhibitory at younger ages than was observed at P17.5. Therefore EPL extract was prepared from early postnatal animals at P8.5 (Fig. 7I-J) and P2.5 (Fig. 7K-L) and tested on the olfactory epithelium explants. The age of P8.5 was chosen because overprojecting axons within the EPL were detected at this age using our methods, but had not been previously detected using other methods (Tenne-Brown et al., 1999). Therefore we considered that repellent molecules may be having an effect at this age. The age of P2.5 was chosen because numerous axons overproject into the EPL at this age and thus we considered that it would be less likely that repellent molecules would be present.

The addition of P8.5 EPL extract resulted in the collapse of many axons (arrows, Fig. 7J). While many axons were obviously inhibited by the P8.5 EPL extract, the extent of axon collapse was not as severe as was observed with P17.5 EPL extract (Fig. 7A-B). Control treatments with normal culture medium, with heat inactivated P8.5 EPL extract or with P8.5 frontal cortex extract showed increased axon outgrowth over the same period (data not shown, but quantification is shown in Fig. 8).

When olfactory epithelium explants were treated with EPL extract from P2.5 animals, the majority of axons appeared to stall (arrows, Fig. 7K-L) rather than retract as observed with the extracts from older ages. The P2.5 extract caused only a small number of axons to retract over the 12 hr incubation period. In olfactory epithelium explants cultured in control culture medium, heat inactivated P2.5 EPL extract, and P2.5 cortex extract, the axon processes extended and continue to grow after 12 hr incubation time (data not shown, quantification is shown in Fig. 8).

The extent of axon collapse in the presence of the EPL extract was quantified by measuring the total length of axons from the explant before and after the treatment. As the extent of axon outgrowth varied between explants at the start of the experiment, the data is presented as percent change in axon length relative to the length at the start of the experiment (Fig. 8). Statistical analysis revealed that the P17.5 EPL extract (n=12) significantly inhibited axon outgrowth in comparison to all other treatments (Fig. 8). In particular, the P17.5 EPL extract resulted in a 42% reduction in the total length of axons compared to before addition of extract to those same explants; and more than 50% reduction in length compared to axons in the medium only control treatment group at the same time point ($p<0.001$, n=13). Unlike

the EPL extract, the axon growth following addition of frontal cortex extracts (n=7-8) or heat inactivated extracts (n=6-7) from different aged animals, or glomerular extract (n=5) from P17.5 animals, were not significantly different from medium-only control (Fig. 8). These data indicate that the preparation of the extract did not result in a toxic response that generally affected axon extension. For extracts from P8.5 animals, the EPL extract (n=10) resulted in a significant reduction in axon length with ~25% reduction in axon length compared to medium only control at the same time point ($p<0.01$; Fig. 8). While the P2.5 EPL extract (n=9) stalled axon outgrowth, the effect was not significantly different (Fig. 8).

During early postnatal development, numerous axons over-project into the EPL. If the EPL was attractive to axons during early development, then it would be expected that axon outgrowth would be significantly greater than controls at P2.5. However as this was not the case, the results indicate that with increasing developmental age, the inner layers of the olfactory bulb have an inhibitory/repellent effect on axon outgrowth from the olfactory epithelium explants. This does not negate the possibility that the EPL is attractive to axon growth, but that the balance of attractive/repulsive factors becomes increasingly in favour of repulsive factors with increasing developmental age.

4. Discussion

We reveal here that the external plexiform layer (EPL) is initially a region in which olfactory sensory axons are able to grow extensively, but that with increasing developmental age, the EPL becomes increasingly inhibitory to axon growth. Primary olfactory axons that over-shoot their target layer and enter the EPL often follow considerable tortuous trajectories that can extend for up to 950 μm through the ventral-dorsal and rostro-caudal planes. The aberrant projecting axons were less numerous with increasing developmental age but were detected up to P17 (Fig. 9) at which point axon outgrowth was significantly inhibited by the EPL in vitro.

While it has been shown previously that ~20% of axons grew past the glomerular layer into deeper layers of the bulb, these errors were not detected after P5 in mouse (Tenne-Brown and Key, 1999) and P9 in rat (Santacana et al., 1992). The absence of targeting errors in the older postnatal animals in the previous studies could be due to the poorer sensitivity of the techniques used. We have used both OMP immunohistochemistry on thick free floating sections and the OMP-ZsGreen mice to detect primary olfactory axons with greater sensitivity. OMP is often considered to be a marker of more mature axons and is expressed at low or negligible levels on immature axons. We have shown that in the transgenic OMP-ZsGreen mice, the ZsGreen protein is expressed in immature neurons that do not express high levels of OMP protein and that some axons that do not seem to express OMP protein immunohistochemically can instead be visualised by the ZsGreen protein. However, it is likely that other immature axons that did not express OMP protein or ZsGreen were not detected and thus the incidence of the over-projection that we report here is likely

to be a conservative measure. Our results not only increase the period in which axons are known to normally over-project but we have also determined that the axons follow extensive trajectories within the EPL. Having a clear understanding of the extent of aberrant axonal projections that normally occur is important for understanding the role of axon guidance molecules in the development of the olfactory system.

The mature olfactory system is noted for its exquisite topographic connectivity which enables mosaically distributed sensory neurons expressing the same odorant receptor to converge on topographically-fixed glomeruli in the olfactory bulb. The sensory axons expressing the same odorant receptor initially converge to a diffuse 50 μm locus (Royal and Key, 1999). Over the next several days these axons condense to form a dense tuft. This initial targeting is certainly more specific than the widespread growth of retinal axons across the surface of the superior colliculus (Simon and O'Leary, 1992). While targeting to a specific topographic site on the surface of the olfactory bulb does appear to be relatively precise, the radial growth of axons is rather inaccurate. As later growing olfactory sensory axons enter the bulb they have to grow radially across the depth of the superficial nerve fibre layer to reach the glomerular layer. During this process about 20% of sensory axons over-shoot their lamina termination zone and continue inappropriately into the underlying EPL (Tenne-Brown and Key, 1999).

It has been suggested that much of the overgrowth in the olfactory bulb could actually represent axons entering the glomeruli from tortuous paths rather than axons growing past the glomerular layer (Treloar et al., 2002). We have demonstrated here that this is

clearly not the case. Many of the over-shooting axons that enter the EPL turn and extend tangentially for long distances through the neuropil of the EPL.

Why is it that axons over-project into the EPL during early development but are then absent from the EPL at later ages? The glomerular layer is the target of the in-growing axons and most likely contains strong attractive cues, however some axons may fail to respond appropriately to those cues and instead respond to attractive cues that are expressed within the EPL. Hence axons are likely to respond to a balance of attractive and repulsive cues of differing strengths. We postulated that either the EPL is attractive to some primary olfactory axons during early development or the EPL becomes inhibitory to the axons with increasing age. The results of the EPL extract assay support the second option: that the EPL becomes inhibitory to axons with increasing age. If the younger age EPL was attractive to axons then we would have observed increased axon growth with the P2.5 EPL extract in our explant assay in comparison to controls. However, we instead found increased inhibition of axon outgrowth with age of the EPL extract, which suggests that inhibitory molecules are more strongly expressed in the EPL in older animals that lead to the reduction of axons within the EPL in later ages (Fig. 9). This does not necessarily indicate that the attractive cues are no longer present, but that the effect of the repulsive cues tips the balance in favour of inhibiting axon extension within the EPL. Alternatively, it could be that receptors for the inhibitory cues are not expressed by axons during early development, but become increasingly expressed in the postnatal animals and adults. However, for the EPL extract assays we used olfactory epithelium explants from the same embryonic age and thus the axons in all the experiments would have expressed the same cohort of axon guidance receptors. As the EPL extract from P8.5 and P17.5

animals caused significant axon retraction, whereas the P2.5 EPL extract did not, it indicates that the axons detect and respond to an inhibitory cue that is increasingly expressed with developmental age.

During development of the olfactory system there is a massive influx of new axons into the olfactory bulb during the first 3 weeks of postnatal life in mice as new glomeruli are formed and existing ones become bigger (LaMantia et al., 1992). A large influx of new neurons also occurs after widespread degeneration of the olfactory epithelium when the newly regenerated neurons send their axons into the bulb. Yet, large numbers of axons are only seen within the EPL during the first postnatal week and while we have now detected numerous axons within the EPL up until P17, it is clear that fewer axons are present within the EPL with increasing age. If the same mechanism operated throughout life that facilitated axon growth into the EPL, then it would be expected that axons would be present in high numbers for the first 3 weeks postnatally and also after widespread regeneration in the adult. In addition, in the healthy normal adult in which neurons are constantly turned over it would be expected that smaller numbers of axons were present in the EPL. However, this is clearly not the case and our results demonstrate that a repulsive mechanism within the EPL operates to prevent axons penetrating the EPL in older animals.

Another contributing factor to the inaccuracy of axon targeting and their penetration of the EPL could be the maturity of axons as determined by the expression of odorant receptors. Some odorant receptors are expressed later in development than others (Tian and Ma, 2008) and the formation of glomeruli occurs at different times. For example, the P2 glomeruli form in the late embryonic period (Royal and Key, 1999)

while the M72 glomeruli form in the first postnatal week (Potter et al., 2001). However, as was considered above for the differential expression of axon guidance receptors, we used the same age explants in the assays and thus the axons would have expressed the same cohort of odorant receptors. Thus while the expression of odorant receptors may be a contributing factor to the incidence of over-projecting axons, our data clearly demonstrate that the EPL becomes increasingly inhibitory over development.

It is also important to consider that the reduction in axon length seen in the EPL extract assay may also be caused primarily by neuronal death rather than an axon repulsion response. The identification of the molecule(s) that is responsible for the repulsive activity within the EPL is the work of future studies, but the potential exists that the molecules within the EPL extract may be directly harmful to the neurons. However, quantification of the survival neurons within the different explant assays was beyond the scope of the project and as we did not any obvious observe cell death we consider it to be an unlikely cause of the axon response detected in the EPL assays.

During development, several molecules have been reported to contribute to guiding olfactory axons to their targets by establishing inhibitory boundaries that prevent axons straying into inappropriate regions. For example, molecules that are expressed within the extracellular matrix such as tenascin and condroitin sulfate proteoglycans have been proposed to form a macromolecular wall that prevents axons penetrating into the deeper layers of the olfactory bulb thus restricting the axons to the glomerular layer during the crucial time of glomerular formation (Gonzalez Mde et al., 1993;

Gonzalez and Silver, 1994; Treloar et al., 2009). However, these cues were reported to be maximally expressed in the late embryonic/early postnatal period. Since we now show that the incidence of over-projecting axons continues into the late postnatal period, these embryonically expressed molecules are therefore not sufficient to restrict all axons. Thus it is likely that the increasingly inhibitory EPL environment that forms in the postnatal animal together with glial boundaries and inhibitory molecules within the extracellular matrix that arise in the embryonic animal act in concert to restrict axons to the glomerular layer during the embryonic to late postnatal period.

We have previously shown that following widespread destruction of the olfactory epithelium in adult mice, the axons of newly regenerated neurons at a population level (e.g. visualized with anti-OMP antibodies) appear to correctly repopulate the glomerular layer, without axons over-projecting into the EPL. However in fact axons of specific odorant receptor types do not always initially target their appropriate glomeruli and instead mis-project into neighbouring glomeruli (St John and Key, 2003). For example, P2 odorant receptor axons tended to project to multiple glomeruli over quite a wide-spread region of the olfactory bulb. While we did not detect P2 axons, or axons stained with anti-OMP antibodies, over-projecting into the EPL in that study it is possible that we had failed to detect over-projecting axons due to limits in the sensitivity of the techniques. Therefore in our current study we repeated the experiment, this time using methimazole to destroy the olfactory epithelium and analysed the axon trajectories in the OMP-ZsGreen mice in order to detect all axons. However, consistent with the P2 study we did not detect over-projecting axons at any stage during the growth of the new axons into the olfactory bulb. These results, together with the previous results (St John and Key, 2003), indicate that despite the

inability of the axons to find their correct topographical targets during regeneration, they do not over-project into the EPL in the adult. Many of the axon guidance molecules such as semaphorins, Ephs, CSPG and galectins that are expressed during development of the olfactory system have distinctly different expression patterns in the adult (Cloutier et al., 2004; Cutforth et al., 2003; Gonzalez Mde et al., 1993; St John et al., 2000; Storan et al., 2004; Treloar et al., 2009). Hence following widespread degeneration in the adult, the new axons often fail to find their appropriate targets. Presumably a mistargeted axon in the adult that is searching for its target glomerulus would have the potential opportunity to enter the EPL. However the presence of inhibitory cues in the EPL of the adult would prevent the axons from entering the EPL. In addition potential boundaries caused by distinct layers of glia together with the molecules within the extracellular matrix (such as condroitin sulfate proteoglycans and tenascin) are likely to act in concert to restrict the regions that axons can penetrate (Gonzalez Mde et al., 1993; Gonzalez and Silver, 1994; Treloar et al., 2009). In contrast, during early development the axons that are searching for their targets are able to enter the EPL since the inhibitory cues are not strongly expressed in the EPL and the inhibitory cues within the extracellular matrix are insufficient to restrict all axons. Thus in the adult, the EPL cues operate effectively to restrict the axons to their appropriate layer, while the lack of axon guidance molecules within the glomerular and nerve fibre layers leads to inaccurate targeting following widespread degeneration in the adult.

The phenotype of primary olfactory axons over-projecting into the EPL has been observed for several different knockouts of axon guidance molecules. Neuropilin-2 (Npn-2) is expressed by olfactory axons and loss of Npn-2 resulted in main olfactory

axons entering the ventral EPL for considerably longer than in controls (Walz et al., 2002), and vomeronasal axons inappropriately entered the main olfactory bulb (Cloutier et al., 2002). Conversely, loss of Sema3F, which is expressed by mitral cells, resulted in axons entering the EPL (Cloutier et al., 2004). Expression of a dominant negative form of neuropilin-1 in chick olfactory sensory neurons resulted in axons entering the telencephalon prematurely and to over-shoot the olfactory bulb (Renzi et al., 2000). In addition, knockout of Close homolog of L1, a member of the L1 family of cell adhesion molecules expressed by olfactory axons (Montag-Sallaz et al., 2002) also resulted in axons over-projecting. However, in all these knockouts it appeared that the over-projection phenotype was delayed and that primary olfactory axons were eventually pruned and removed from the EPL such that in the adult the phenotypes were not observed. Thus it may be that there is a combination of molecules that act together to repel axons from the EPL and loss of any one of these molecules is insufficient to overcome the combined repellent activity that occurs in older animals.

Several putative axon repellent molecules are expressed in the olfactory bulb such as Eph receptors (EphA5 and EphA3 on mitral cells; Cooper et al., 2009; Cutforth et al., 2003) and ephrin ligands (ephrin-A5 is expressed at low levels on mitral cells; St John et al., 2002; St John et al., 2000). In addition, semaphorins are expressed in subsets of mitral and periglomerular cells (Giger et al., 1998). Knockout of ephrinA3 and ephrinA5 has been reported to affect primary olfactory axon targeting (Cutforth et al., 2003), however the trajectory of individual axons was not reported perhaps because the sensitive techniques such as we have used to detect individual axons were not available; hence it is possible that over-projecting axons were also present in these

knockout mice. Unfortunately Eph/ephrins are also expressed on primary olfactory axons (Cutforth et al., 2003; St John et al., 2000) and we have previously shown that activation of EphA5 inhibits olfactory sensory axon outgrowth in vitro (St John et al., 2000). We were therefore unable to test the role of Eph/ephrins in our current assays with respect to their role in the EPL, since it would be unclear whether the response was due to Ephs/ephrins arising from the EPL or Ephs/ephrins that are expressed by the axons themselves. Hence the role of the Eph/ephrins within the EPL can only be examined by perturbing their expression specifically on mitral cells but this is beyond the scope of the current project.

The over-shooting of axons into the EPL is likely to be regulated in part by other mechanisms such as activity dependent pruning and retraction of axons. In mice lacking adenylyl cyclase 3 there is increased over-shooting up to 20 days postnatal development (Zou et al., 2007). Interestingly, this activity dependent property may itself be associated with changes in the expression of the chemorepulsive receptor neuropilin-1 (Zou et al., 2007). In addition, knockout of the olfactory cyclic nuecleotide-gated channel subunit 1 in mice resulted in a small number of primary olfactory axons over-projecting into the EPL, although the extent of the trajectories of the over-projecting axons was not clear (Baker et al., 1999). This indicates that signal transduction via OCNC1 may be important for maintaining primary olfactory axons within their glomerular targets. However, it was also noted in these mice that the olfactory receptor neurons appeared to have delayed maturation as indicated by a lack of expression of OMP. We have previously shown that in mice lacking OMP, that primary olfactory sensory axons over-project into the EPL (St John and Key, 2005) consistent with the OCNC1 knockout phenotype. Thus in the OCNC1 knockout mice

it is unclear whether it is the loss of OCNC1 or the lack of OMP expression that results in axons over-projecting into the EPL.

In summary, we demonstrate that many olfactory sensory axons naturally over-shoot the glomerular layer up until two-three weeks postnatally. During early development, the axons are able to grow extensively within the EPL along the ventro-dorsal and rostro-caudal axes of the bulb with some trajectories up to at least 950 μm. However, the EPL becomes increasingly inhibitory to axon growth during later development which indicates that chemorepulsive molecules that are expressed in the deeper layers of the bulb inhibit axon growth within the EPL. Future work will characterize the molecules that contribute to the repellent activity present within the EPL.

5. Acknowledgements

This work was supported by grants from the National Health and Medical Research Council to J.St.J and B.K (grant numbers 511006) and by funding to the National Centre for Adult Stem Cell Research from the Australian Government Department of Health and Aging (A.M.S.), and an Australian Postgraduate Award to L.W. We thank Professor Frank Margolis for providing the antibodies against OMP.

6. References

Bagnard, D., Chounlamountri, N., Puschel, A.W., Bolz, J., 2001. Axonal surface molecules act in combination with semaphorin 3a during the establishment of corticothalamic projections. Cereb Cortex 11, 278-285.

Bailey, M.S., Puche, A.C., Shipley, M.T., 1999. Development of the olfactory bulb: evidence for glia-neuron interactions in glomerular formation. J Comp Neurol 415, 423-448.

Baker, H., Cummings, D.M., Munger, S.D., Margolis, J.W., Franzen, L., Reed, R.R., Margolis, F.L., 1999. Targeted deletion of a cyclic nucleotide-gated channel subunit (OCNC1): biochemical and morphological consequences in adult mice. J Neurosci 19, 9313-9321.

Brittebo, E.B., 1995. Metabolism-dependent toxicity of methimazole in the olfactory nasal mucosa. Pharmacology & toxicology 76, 76-79.

Cloutier, J.F., Giger, R.J., Koentges, G., Dulac, C., Kolodkin, A.L., Ginty, D.D., 2002. Neuropilin-2 mediates axonal fasciculation, zonal segregation, but not axonal convergence, of primary accessory olfactory neurons. Neuron 33, 877-892.

Cloutier, J.F., Sahay, A., Chang, E.C., Tessier-Lavigne, M., Dulac, C., Kolodkin, A.L., Ginty, D.D., 2004. Differential requirements for semaphorin 3F and Slit-1 in axonal targeting, fasciculation, and segregation of olfactory sensory neuron projections. J Neurosci 24, 9087-9096.

Cooper, M.A., Crockett, D.P., Nowakowski, R.S., Gale, N.W., Zhou, R., 2009. Distribution of EphA5 receptor protein in the developing and adult mouse nervous system. J Comp Neurol 514, 310-328.

Cutforth, T., Moring, L., Mendelsohn, M., Nemes, A., Shah, N.M., Kim, M.M., Frisen, J., Axel, R., 2003. Axonal ephrin-As and odorant receptors: coordinate determination of the olfactory sensory map. Cell 114, 311-322.

Danciger, E., Mettling, C., Vidal, M., Morris, R., Margolis, F., 1989. Olfactory marker protein gene: its structure and olfactory neuron-specific expression in transgenic mice. Proc Natl Acad Sci U S A 86, 8565-8569.

Devine, C.A., Key, B., 2008. Robo-Slit interactions regulate longitudinal axon pathfinding in the embryonic vertebrate brain. Dev Biol 313, 371-383.

Dynes, J.L., Ngai, J., 1998. Pathfinding of olfactory neuron axons to stereotyped glomerular targets revealed by dynamic imaging in living zebrafish embryos. Neuron 20, 1081-1091.

Giger, R.J., Pasterkamp, R.J., Heijnen, S., Holtmaat, A.J., Verhaagen, J., 1998. Anatomical distribution of the chemorepellent semaphorin III/collapsin-1 in the adult rat and human brain: predominant expression in structures of the olfactory-hippocampal pathway and the motor system. J Neurosci Res 52, 27-42.

Gonzalez Mde, L., Malemud, C.J., Silver, J., 1993. Role of astroglial extracellular matrix in the formation of rat olfactory bulb glomeruli. Experimental neurology 123, 91-105.

Gonzalez, M.L., Silver, J., 1994. Axon-glia interactions regulate ECM patterning in the postnatal rat olfactory bulb. J Neurosci 14, 6121-6131.

Graziadei, G.A., Stanley, R.S., Graziadei, P.P., 1980. The olfactory marker protein in the olfactory system of the mouse during development. Neuroscience 5, 1239-1252.

Hindges, R., McLaughlin, T., Genoud, N., Henkemeyer, M., O'Leary, D.D., 2002. EphB forward signaling controls directional branch extension and arborization required for dorsal-ventral retinotopic mapping. Neuron 35, 475-487.
Kapfhammer, J.P., Xu, H., Raper, J.A., 2007. The detection and quantification of growth cone collapsing activities. Nature protocols 2, 2005-2011.
Keller, A., Margolis, F.L., 1975. Immunological studies of the rat olfactory marker protein. J Neurochem 24, 1101-1106.
Key, B., Akeson, R.A., 1993. Distinct subsets of sensory olfactory neurons in mouse: possible role in the formation of the mosaic olfactory projection. J Comp Neurol 335, 355-368.
Klenoff, J.R., Greer, C.A., 1998. Postnatal development of olfactory receptor cell axonal arbors. J Comp Neurol 390, 256-267.
LaMantia, A.S., Pomeroy, S.L., Purves, D., 1992. Vital imaging of glomeruli in the mouse olfactory bulb. J Neurosci 12, 976-988.
Matz, M.V., Fradkov, A.F., Labas, Y.A., Savitsky, A.P., Zaraisky, A.G., Markelov, M.L., Lukyanov, S.A., 1999. Fluorescent proteins from nonbioluminescent Anthozoa species. Nature biotechnology 17, 969-973.
Mombaerts, P., 1996. Targeting olfaction. Curr Opin Neurobiol 6, 481-486.
Montag-Sallaz, M., Schachner, M., Montag, D., 2002. Misguided axonal projections, neural cell adhesion molecule 180 mRNA upregulation, and altered behavior in mice deficient for the close homolog of L1. Mol Cell Biol 22, 7967-7981.
Ozaki, S., Snider, W.D., 1997. Initial trajectories of sensory axons toward laminar targets in the developing mouse spinal cord. J Comp Neurol 380, 215-229.
Poeck, B., Fischer, S., Gunning, D., Zipursky, S.L., Salecker, I., 2001. Glial cells mediate target layer selection of retinal axons in the developing visual system of Drosophila. Neuron 29, 99-113.
Potter, S.M., Zheng, C., Koos, D.S., Feinstein, P., Fraser, S.E., Mombaerts, P., 2001. Structure and emergence of specific olfactory glomeruli in the mouse. The Journal of Neuroscience 21, 9713-9723.
Renzi, M.J., Wexler, T.L., Raper, J.A., 2000. Olfactory sensory axons expressing a dominant-negative semaphorin receptor enter the CNS early and overshoot their target. Neuron 28, 437-447.
Ressler, K.J., Sullivan, S.L., Buck, L.B., 1993. A zonal organization of odorant receptor gene expression in the olfactory epithelium. Cell 73, 597-609.
Ressler, K.J., Sullivan, S.L., Buck, L.B., 1994. Information coding in the olfactory system: evidence for a stereotyped and highly organized epitope map in the olfactory bulb. Cell 79, 1245-1255.
Royal, S.J., Key, B., 1999. Development of P2 olfactory glomeruli in P2-internal ribosome entry site-tau-LacZ transgenic mice. J Neurosci 19, 9856-9864.
Santacana, M., Heredia, M., Valverde, F., 1992. Transient pattern of exuberant projections of olfactory axons during development in the rat. Brain Res Dev Brain Res 70, 213-222.
Silos-Santiago, I., Jeng, B., Snider, W.D., 1995. Sensory afferents show appropriate somatotopy at the earliest stage of projection to dorsal horn. Neuroreport 6, 861-865.
Simon, D.K., O'Leary, D.D., 1992. Development of topographic order in the mammalian retinocollicular projection. J Neurosci 12, 1212-1232.
St John, J.A., Key, B., 2003. Axon Mis-targeting in the Olfactory Bulb During Regeneration of Olfactory Neuroepithelium. Chem Senses 28, 773-779.

St John, J.A., Key, B., 2005. Olfactory marker protein modulates primary olfactory axon overshooting in the olfactory bulb. J Comp Neurol 488, 61-69.
St John, J.A., Pasquale, E.B., Key, B., 2002. EphA receptors and ephrin-A ligands exhibit highly regulated spatial and temporal expression patterns in the developing olfactory system. Brain Res Dev Brain Res 138, 1-14.
St John, J.A., Tisay, K.T., Caras, I.W., Key, B., 2000. Expression of EphA5 during development of the olfactory nerve pathway in rat. J Comp Neurol 416, 540-550.
Storan, M.J., Magnaldo, T., Biol-N'Garagba, M.C., Zick, Y., Key, B., 2004. Expression and putative role of lactoseries carbohydrates present on NCAM in the rat primary olfactory pathway. J Comp Neurol 475, 289-302.
Tenne-Brown, J., Key, B., 1999. Errors in lamina growth of primary olfactory axons in the rat and mouse olfactory bulb. J Comp Neurol 410, 20-30.
Tian, H., Ma, M., 2008. Differential development of odorant receptor expression patterns in the olfactory epithelium: a quantitative analysis in the mouse septal organ. Dev Neurobiol 68, 476-486.
Treloar, H., Tomasiewicz, H., Magnuson, T., Key, B., 1997. The central pathway of primary olfactory axons is abnormal in mice lacking the N-CAM-180 isoform. J Neurobiol 32, 643-658.
Treloar, H., Walters, E., Margolis, F., Key, B., 1996. Olfactory glomeruli are innervated by more than one distinct subset of primary sensory olfactory neurons in mice. J Comp Neurol 367, 550-562.
Treloar, H.B., Feinstein, P., Mombaerts, P., Greer, C.A., 2002. Specificity of glomerular targeting by olfactory sensory axons. J Neurosci 22, 2469-2477.
Treloar, H.B., Purcell, A.L., Greer, C.A., 1999. Glomerular formation in the developing rat olfactory bulb. J Comp Neurol 413, 289-304.
Treloar, H.B., Ray, A., Dinglasan, L.A., Schachner, M., Greer, C.A., 2009. Tenascin-C is an inhibitory boundary molecule in the developing olfactory bulb. J Neurosci 29, 9405-9416.
Vassar, R., Chao, S.K., Sitcheran, R., Nunez, J.M., Vosshall, L.B., Axel, R., 1994. Topographic organization of sensory projections to the olfactory bulb. Cell 79, 981-991.
Walz, A., Rodriguez, I., Mombaerts, P., 2002. Aberrant sensory innervation of the olfactory bulb in neuropilin-2 mutant mice. J Neurosci 22, 4025-4035.
Wang, F., Nemes, A., Mendelsohn, M., Axel, R., 1998. Odorant receptors govern the formation of a precise topographic map. Cell 93, 47-60.
Wenck, A., Pugieux, C., Turner, M., Dunn, M., Stacy, C., Tiozzo, A., Dunder, E., van Grinsven, E., Khan, R., Sigareva, M., Wang, W.C., Reed, J., Drayton, P., Oliver, D., Trafford, H., Legris, G., Rushton, H., Tayab, S., Launis, K., Chang, Y.F., Chen, D.F., Melchers, L., 2003. Reef-coral proteins as visual, non-destructive reporters for plant transformation. Plant cell reports 22, 244-251.
Windus, L.C., Lineburg, K.E., Scott, S.E., Claxton, C., Mackay-Sim, A., Key, B., St John, J.A., 2010. Lamellipodia mediate the heterogeneity of central olfactory ensheathing cell interactions. Cell Mol Life Sci 67, 1735-1750.
Yates, P.A., Roskies, A.L., McLaughlin, T., O'Leary, D.D., 2001. Topographic-specific axon branching controlled by ephrin-as is the critical even in retinotectal map development. The Journal of Neuroscience 21, 8548-8563.
Zou, D.J., Chesler, A.T., Le Pichon, C.E., Kuznetsov, A., Pei, X., Hwang, E.L., Firestein, S., 2007. Absence of adenylyl cyclase 3 perturbs peripheral olfactory projections in mice. J Neurosci 27, 6675-6683.

7. Figure legends

Figure 1. Parasagittal sections reveal extent of axon trajectories within the external plexiform layer. (A) Coronal section of P0.5 mouse olfactory bulb immunoreacted with antibodies against OMP. Numerous axons penetrated the external plexiform layer (EPL) with some axons forming aggregrates (arrows) within the EPL. (B) Higher power view of axons within the EPL. These axons appeared to project short distances and often looped back (arrows) towards the glomerular layer (GL). Occasionally axons projected past the mitral cell layer (ML) into the internal plexiform layer (arrowhead). (C) Parasagittal sections (100 μm) of mouse olfactory bulbs and cortex were cut (dashed line) to provide flat-mount sections of the EPL. (D) Medial parasagittal sections (dashed line) were cut through extensive areas of the EPL, whereas other parasagittal sections (dotted line) passed through central regions of the bulb. (E) Immunohistochemistry using antibodies against OMP in a glancing section through the EPL of P0.5 olfactory bulb revealed extensive projections (arrows) of primary olfactory axons within the EPL; vGL = ventral glomerular layer, dGL = dorsal glomerular layer. (F) Higher power view of E; vGL is slightly in view at the bottom left, dGL is out of view but indicated by the arrow. E-F are parasagittal sections with rostral to the left and dorsal to the top. Scale bar is 125 μm in A, D; 50 μm in B; 250 μm in C,E; 100 μm in F.

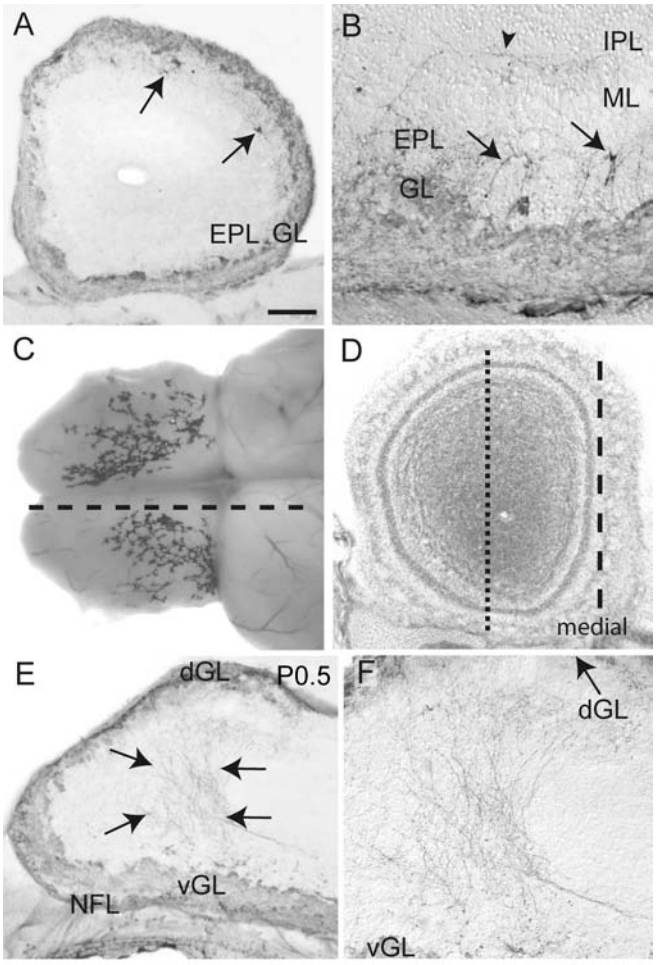
A
EPL GL
B
IPL
ML
EPL
GL
C
D
medial
E
dGL
P0.5
NFL
vGL
F
dGL
vGL

Figure 2 Primary olfactory axons project vast distances within the external plexiform layer. Panels show parasagittal sections through the EPL with rostral to the left and dorsal to the top. (A-B) Numerous primary olfactory axons were present within the EPL at P6.5 (A) and at P8.5 (B); boxed area in B is shown in E. C-E are montages of higher magnification views of the axon projections within the EPL. (C) At P4.5, axons were observed coursing throughout the EPL with some axons projecting extensive distances. (D) In a P6.5 animal, the trajectory of an individual axon (dashed line) projected over more than half the dorso-ventral width of the olfactory bulb, before disappearing out of the plane of the section. (E) A montage of different focal planes demonstrating the trajectory of numerous axons in a single section through the EPL of a P8.5 olfactory bulb. Scale bar is 250 μm in A-B; 75 μm in C-E.

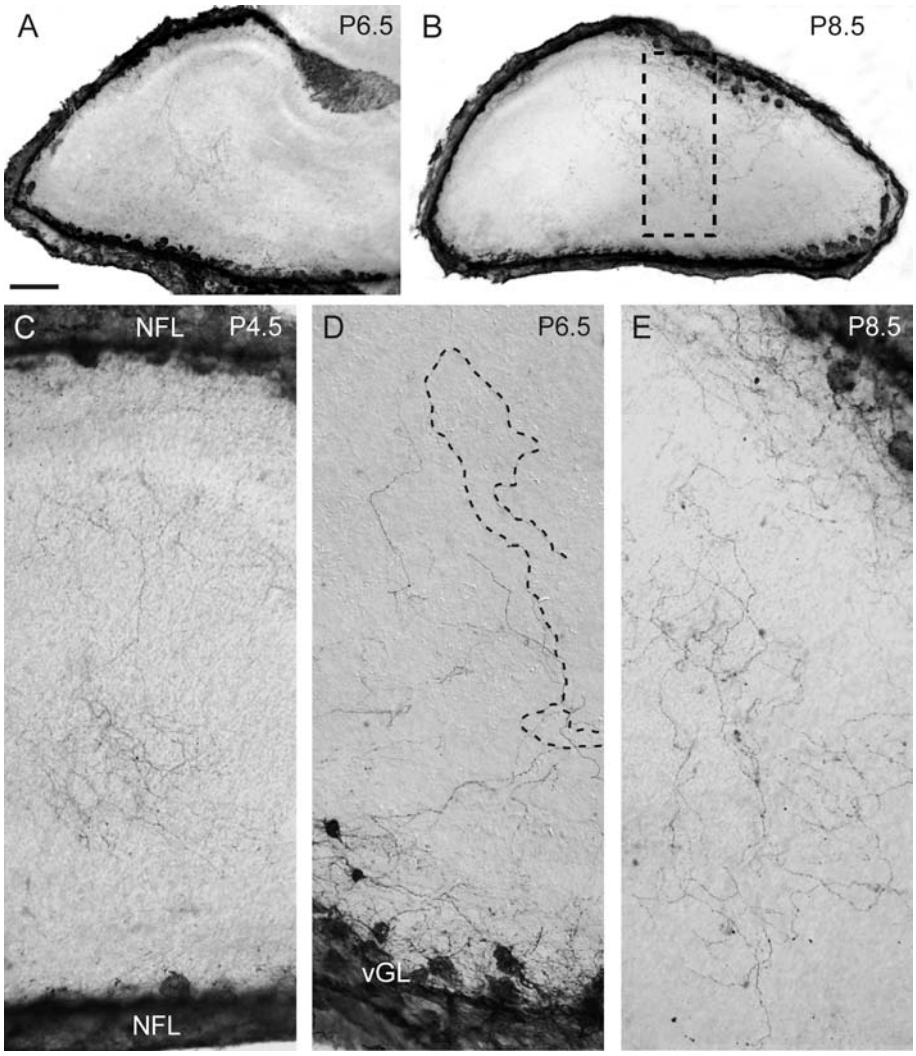

Figure 3. Primary olfactory axons form an extensive network with the external plexiform layer. Parasagittal sections that passed through the middle portion of the olfactory bulb revealed the longitudinal aspect of the EPL as well as the mitral cell (ML) and granule cell layers. (A-F) axon projections in Quackenbush mice. (A) At P6.5, numerous primary olfactory axons were detected projecting past the glomerular layer (GL) into the EPL and extending in the rostro-caudal plane (open arrowheads). Occasionally axons (arrow) projected past the ML but usually looped back into the EPL. (B, D) Extensive axonal projections into the EPL continued to be present at P8.5. (E) By P11.5, fewer axons (open arrowheads) projected into the EPL. (C) A low power image of the main and accessory olfactory bulb in a P6.5 animal showing staining of the lectin DBA. The accessory olfactory bulb (AOB) was strongly stained while some scattered glomeruli (arrowheads) of the main olfactory bulb also were labelled by DBA with only a few main olfactory glomeruli (unfilled arrowheads) being close to the AOB. (F) A higher magnification view of the AOB shows that DBA-labelled accessory olfactory axons (arrows) projected into the plexiform layer of the AOB. Scale bar is 50 μm in A,B,D,E; 650 μm in C; 175 μm in F.

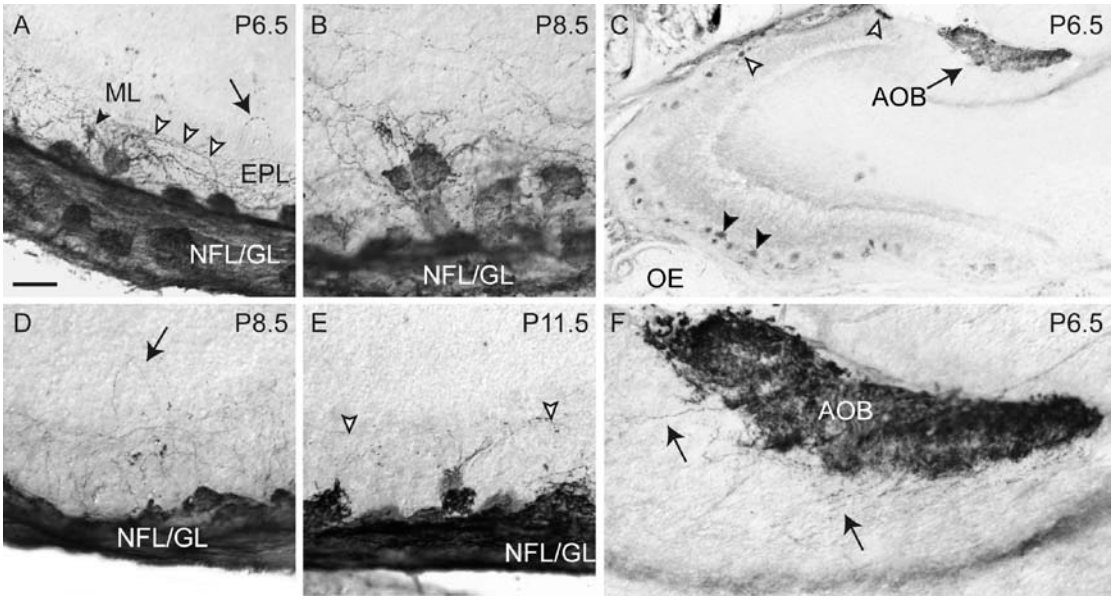

Figure 4. OMP-ZsGreen transgenic mice provide excellent visualisation of primary olfactory axons. (A) In a coronal section of a P14 animal, primary olfactory neurons throughout the olfactory epithelium expressed ZsGreen. (B) The neurons expressed ZsGreen along the length of the axons including within glomeruli of the olfactory bulb in P2.5 animals. (C) A higher power view of the image shown in B. (D) In the olfactory epithelium of P7 OMP-ZsGreen transgenic mice, primary olfactory neurons expressed ZsGreen protein in the soma, dendrites and axons. Weak ZsGreen expression was also observed in immature neurons (arrow). (E) Anti-OMP immunohistochemistry of the section shown in D; weak immunostaining was present in immature neurons (arrow). (F) Double labelling revealed the vast majority of olfactory neurons expressed ZsGreen together with OMP, with axons (arrow) being clearly labelled in the lamina propria (LP). (G) Secondary-only control of olfactory epithelium. (H) In the olfactory bulb of P7 OMP-ZsGreen transgenic mice, primary olfactory axons were clearly visible over-projecting into the external plexiform layer (EPL). (I) Anti-OMP immunohistochemistry of the section shown in G. (J) Double labelling revealed that the visualisation of primary olfactory axons by ZsGreen expression was more robust than by detection using anti-OMP immunohistochemistry with some axons expressing ZsGreen (arrow) but having limited levels of anti-OMP immunofluorescence. (K) Secondary-only control of EPL and glomerular layer. Scale bar is 625 μm in A; 315 μm in B; 60 μm in C; 100 μm in D-G; 35 μm in H-K.

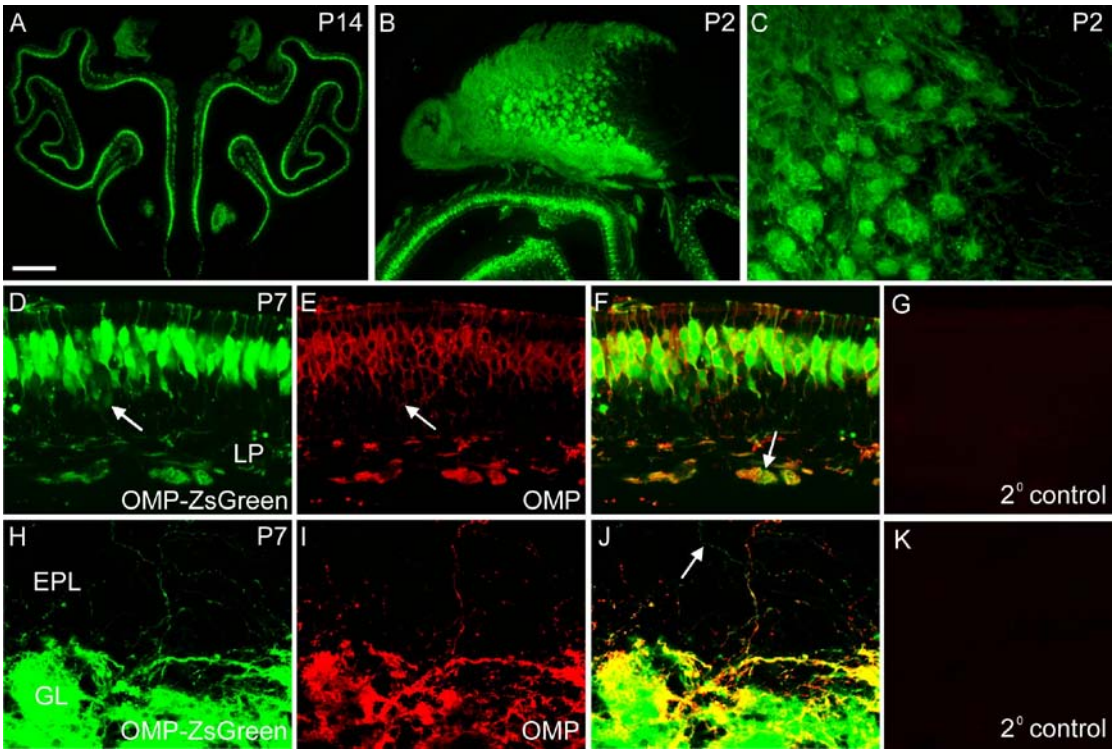

Figure 5. Primary olfactory axons trajectories in OMP-ZsGreen transgenic mice. (A) In glancing sections of the EPL, primary olfactory axons that expressed ZsGreen displayed extensive trajectories at P2.5 similar to those detected by DAB immunostaining (see Figs. 1-2). (B) Higher power view of A. (C) In parasagittal sections of P2.5 animals, axons that projected past the glomerular layer had trajectories with a distinct caudal preference; this section had only a small region of EPL and hence the axon trajectories appear short. (D) In a glancing section through the EPL in P7 animals, individual axons projected for at least one-third of the rostral caudal distance of the olfactory bulb. Iindividual axons can be seen in the boxed area that is shown in E. (E) A single primary olfactory axon (arrow) projected into the EPL of a P7 animal for at least 850 μm. (F) In sections of other P7 animals, the numerous axons (arrows) made it difficult to track the trajectory of individual axons within the EPL. (G) In coronal sections of P7 animals, the trajectories of axons (arrow) could only be tracked for a short distance; green fluorescent dots may indicate axons projecting in the rostral-caudal plane (arrowhead). (H-I) At P17, axons (arrows)

continued to be detected within the EPL. (J) Quantification of the percentage area covered by ZsGreen axons within the EPL in P2 and P2 animals; $p<0.001$, n=3 animals. (K) Quantification of the breadth of the EPL in the coronal plane (n=13 for both P2 and P7) and in the sagittal plane (n=17 for both P2 and P7) and the distance of the trajectory of axons within the EPL in the coronal plane of P2 (n=46 axons) and P7 (n=52 axons) animals and in the sagittal plane of P2 (n=66 axons) and P7 (n=119 axons) animals. Data is presented as a box and whisker plot; *** $p<0.001$. Scale bar is 250 μm in A; 100 μm in B; 25 μm in C; 350 μm in D; 70 μm in E-G; 50 μm in H-I.

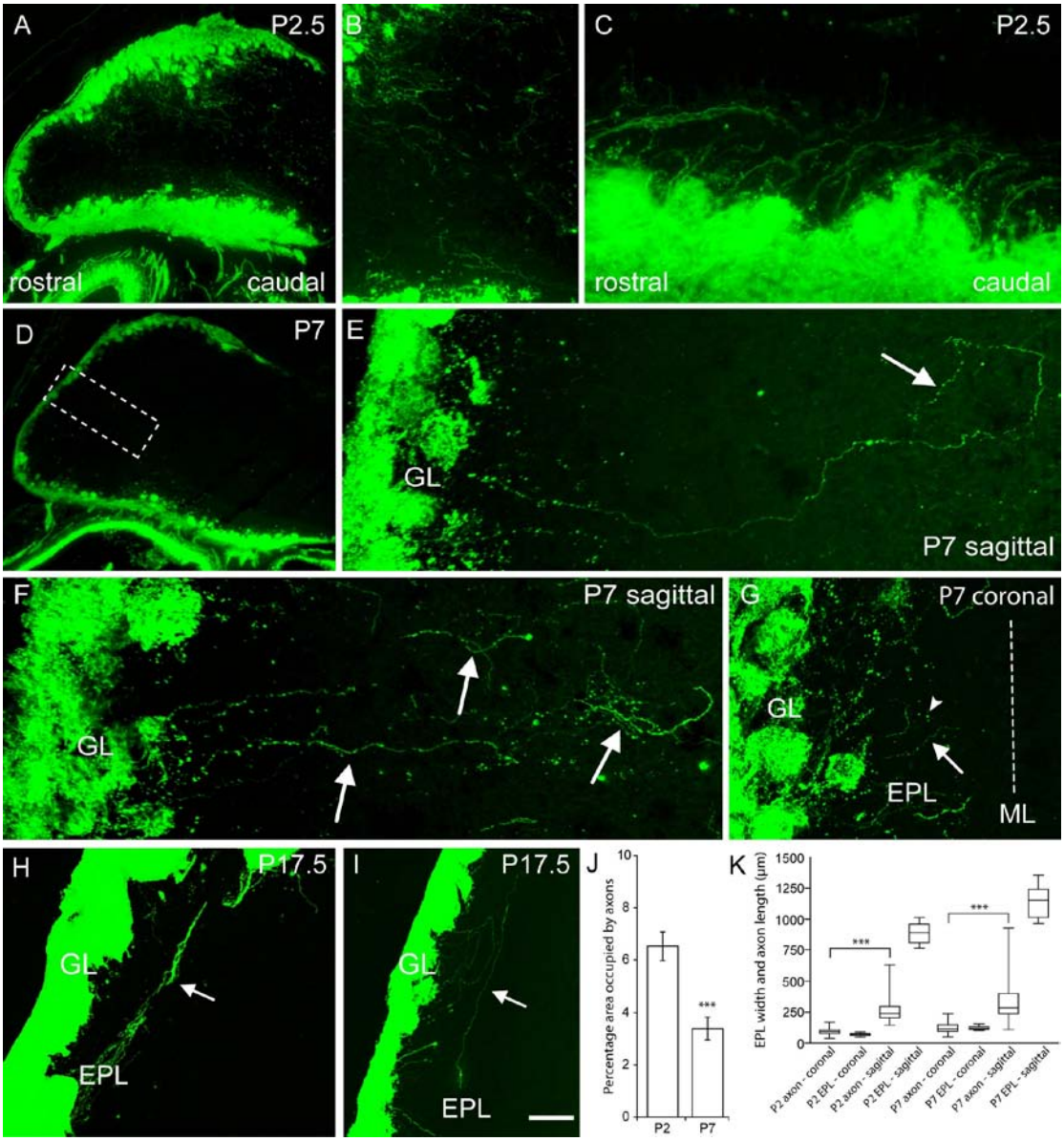

Figure 6. Axons do not over-project after large scale degeneration. Adult OMP-ZsGreen mice were treated with methimazole to cause degeneration of the olfactory epithelium. Panels A-D show images with both fluorescence and DIC; E-H show fluorescence only; sections are in the coronal plane. (A) Three days following treatment, the apical layer olfactory epithelium (arrow) was shed into the nasal cavity (NC) leaving the basal layer intact (demarcated by the dotted line). (B-D) 7-21 days following treatment, the olfactory epithelium including primary olfactory sensory neurons (green) regenerated. (E-H) In the olfactory bulb, primary sensory axons terminated in glomeruli (dashed circles) and did not over-project into the external plexiform layer (EPL) at any stage following methimazole treatment. Arrow in E points to macrophages that accumulated axonal debris. GL, glomerular layer; LP, lamina propria; NFL, nerve fibre layer; OE, olfactory epithelium. Scale bar is 50 μm in A-D; 75 μm in E-H.

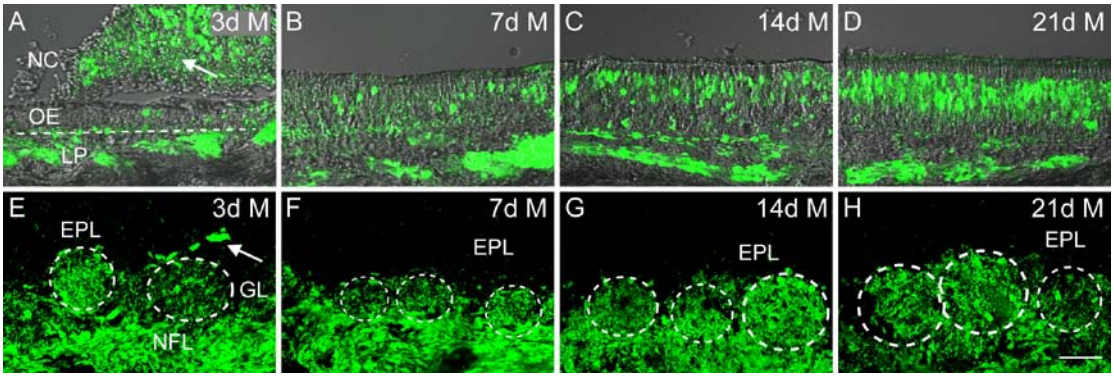

Figure 7. Axon collapse is induced by extract from the inner layer of olfactory bulb. Olfactory epithelium (OE) explants were prepared from E14.5 OMP-ZsGreen embryos, cultured for 2 days and then incubated with extract for 12 hr. (A-B) Extract prepared from the inner layer of P17.5 olfactory bulb (EPL extract) was added to the OE explant. (C-D) Normal complete growth medium. (E-F) Heat inactivated (70 ^{o}C for 20 min) P17.5 EPL extract. (G-H) Extract prepared from the frontal cortex of

P17.5 animals. (I-J) Extract from P8.5 EPL. (K-L) Extract from P2.5 EPL. Arrows indicate axon collapse; arrowheads indicate axon extension. Scale bar = 200 μm.

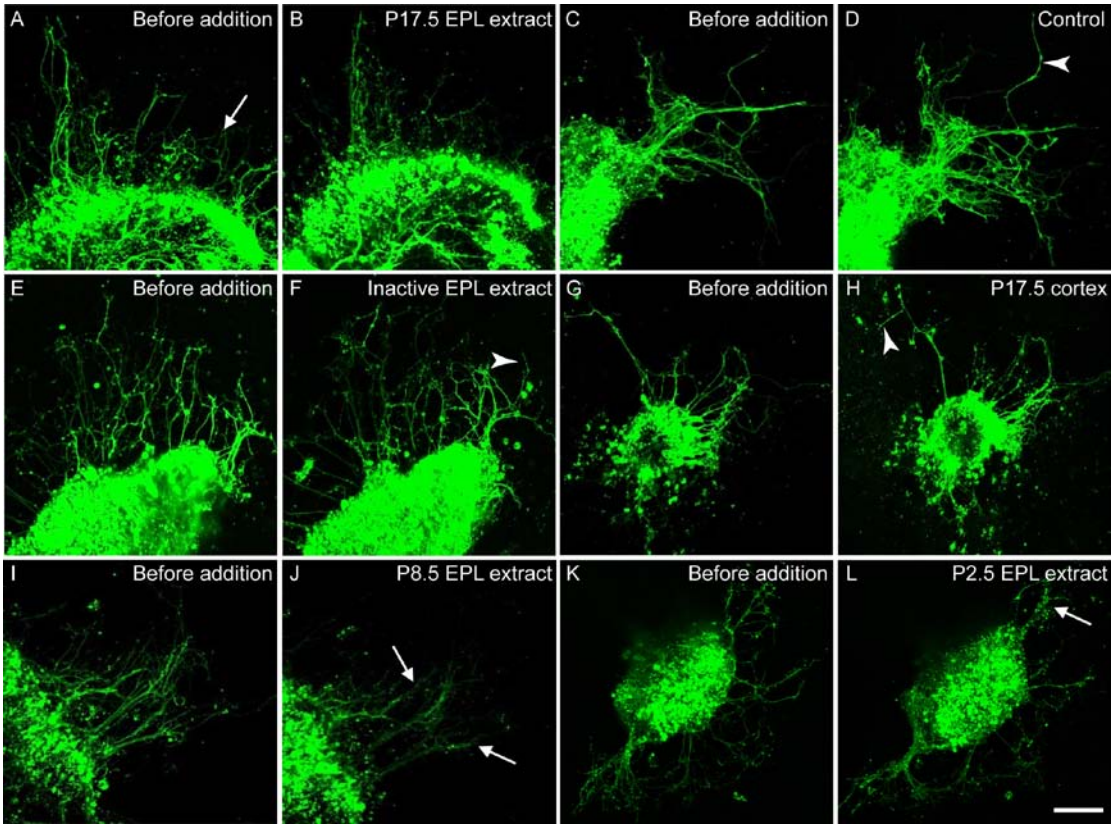

Figure 8. EPL extract inhibits growth of primary olfactory axons. Quantification of axon outgrowth from OE explants. N values represents the number of explants, with 3 repeats being performed with at least 2-3 explants per experiment. Explants were cultured in the presence of culture medium only (n=13 explants); EPL extracts from P2.5 (n=9 explants), P8.5 (n=10 explants) and P17.5 (n=12 explants) animals and cortex extracts from P2.5 (n=7 explants), P8.5 (n=7 explants) and P17.5 (n=8 explants) animals; glomerular extract from P17.5 animals (n=5); heat inactivated EPL extract from P2.5 (n=6 explants), P8.5 (n=6 explants) and P17.5 (n=7 explants) animals. Axon lengths were measured at t=0 and then the change in lengths were determined after 12 hr incubation; a zero percentage change means the axons did not change in length; a 10% change means they increased in size by an additional 10%.

p<0.001 Kruskal-Wallis test and *p<0.05, **p<0.01 and ***p<0.001 post-hoc Dunnnett's Multiple Comparison test. The P17.5 EPL extract data was significantly different from all other groups, but the significance level is only shown for select

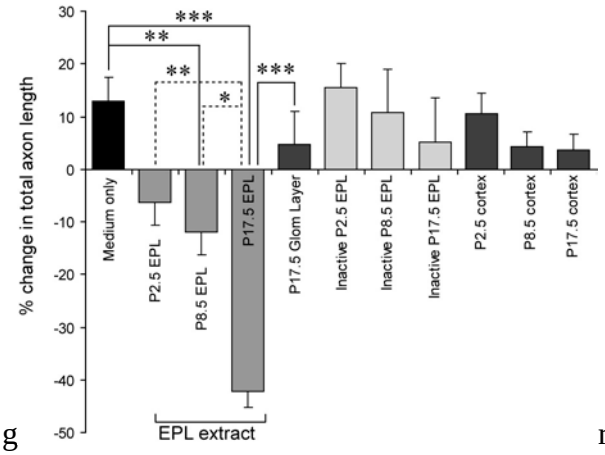

groups.

Figure 9. Primary olfactory axons have extensive trajectories within the EPL, but are repelled from the layer with increasing developmental age. (A) In coronal sections, the apparent extent of the trajectories of axons is restricted by the plane of section. (B) Parasagittal sections through the EPL to provide slices of the full width of the EPL reveal the trajectory of the axons. (C-E) When viewed in parasagittal sections of the EPL, it is clear that axons that enter the EPL in the early postnatal period can have extensive trajectories which tend to project dorsally and caudally. With increasing developmental age, the EPL becomes inhibitory to axon growth and axons are lost from the EPL although some axons do continue to persist within the EPL up to P17. NC, nasal cavity; Cx, cortex.